Influence of penetration enhancer isopropyl myristate to stratum corneum lipid model membranes revealed by neutron diffraction and ^{2}H NMR experiments

Adina Eichner[1], Sören Stahlberg[2], Stefan Sonnenberger[1], Bodo Dobner[1], Andreas Ostermann[3], Tobias E. Schrader[4], Thomas Haußß[5], Annett Schroeter[6], Daniel Huster[2], Reinhard H. H. Neubert[1,7]

[1] Institute of Pharmacy, Martin Luther University Halle-Wittenberg, 06120 Halle/Saale, Germany

[2] Institute of Medical Physics and Biophysics, University of Leipzig, 04107 Leipzig, Germany

[3] Heinz Maier-Leibnitz Zentrum (MLZ), Technische Universität München, 85747 Garching, Germany

[4] Jülich Centre for Neutron Science (JCNS) at Heinz Maier-Leibnitz Zentrum (MLZ), Forschungszentrum Jülich GmbH, 85748 Garching, Germany

[5] Institute of Soft Matter and Functional Materials, Helmholtz-Zentrum Berlin für Materialien und Energie, 14109 Berlin, Germany

[6] DR.KADE Pharmazeutische Fabrik GmbH, 12277 Berlin, Germany

[7] Institute of Applied Dermatopharmacy at the Martin Luther University Halle-Wittenberg, 06120 Halle/Saale, Germany

KEYWORDS: Stratum corneum, Lipid model membranes, Ceramides, Penetration enhancer, Neutron diffraction, ^{2}H solid-state NMR spectroscopy, Phase transition

ABBREVIATIONS AND SYMBOLS

b_{coh}	Coherent neutron scattering lengths
d/D	Deuterium
d	d-spacing (lamellar repeat distance)
Fh, SF	Structure factor
LPP	Long periodicity phase
SPP	Short periodicity phase

ABSTRACT

The outermost layer of mammalian skin is the stratum corneum (SC), which provides the main barrier property. The barrier function is attributed to the intercellular lipids, forming continuous multilamellar membranes. In this study, SC lipid model membranes enriched with deuterated lipids were analyzed by neutron diffraction and ^{2}H solid-state NMR spectroscopy. Especially the effect of the penetration enhancer isopropyl myristate (IPM) on a well-known SC lipid model membrane containing synthetically derived methyl-branched ceramide [EOS], a short-chain ceramide [AP], behenic acid and cholesterol was focused. To this end, for the first time, the neutron diffraction instrument BIODIFF (Heinz Maier-Leibnitz Zentrum, Garching, Germany) was used for investigations on biological skin models. IPM supported the formation of a single short periodicity phase (SPP), in which we determined the position of CER[AP] and the absence of long-chain CER[EOS]. Furthermore, the thermotropic phase behavior of the lipid system was analyzed by additional neutron diffraction studies as well as ^{2}H solid-state NMR spectroscopy, covering temperatures of 32°C (physiological skin temperature), 50 °C, 70 °C and a subsequent cooldown back to skin temperature. We found a phase transition and a hysteresis effect of the lipids with both techniques. During the cooldown Bragg peaks corresponding to a long periodicity phase (LPP) appeared. Additionally, ^{2}H NMR revealed that IPM molecules show isotropic phase behavior at all temperatures.

INTRODUCTION

Being the uppermost and thinnest of all skin layers, the stratum corneum (SC) maintains an important function as main barrier for penetrating substances [1, 2]. Due to its complex structure, it is not only able to protect the body from external influences but also prevents dehydration as it controls transepidermal water loss (TEWL). Both mechanisms are primarily attributed to the intercellular lipids, which surround the dead corneocytes and form complex multilamellar membranes [3]. It is well established that the structural organization of these layers determines the SC barrier [1] but is not yet fully understood. Simultaneously, the major pathway of skin penetrating substances leads through this SC lipid matrix [3].

The major lipid classes abundant in the SC lipid matrix are ceramides (CER), cholesterol (CHOL) and free fatty acids (FFA) [3-5]. Among these, the very heterogeneous group of CER is known to play a fundamental role for the structural arrangement, and hence for the maintenance of the barrier function of the skin [6]. The large amount of sphingolipids constitutes the main part of the matrix ingredients [7]. As many as 342 individual compounds have lately been described [8] involving all subspecies, which are classified into 19 classes [8-11]. Their quantification [12-16] as well as their molecular arrangement [17-19] were subjects in numerous studies. Based on that high number of different molecules, individual interactions between CER subspecies and the lamellar lipid structure became a central point of interest.

Lipids extracted from native SC are able to form two lamellar phases: a short periodicity phase (SPP) with an approximated spacing of 60 Å and a long periodicity phase (LPP) with a repeat interval of 130 Å [20-22]. The SPP is known to be mostly determined by the short chain lipids such as CER[AP] or [NP] [23, 24], the LPP is connected to the long-chain CER such as [EOS] [25-29]. Whereas the SPP is well defined by neutron diffraction studies [23, 30-33], the existence of its longer pendant is still under discussion. In 1987, a first study was published by Madison et al., where the authors were able to determine a large lamellar phase with a repeat distance of 130 Å [20]. This was confirmed by Bouwstra et al. on human skin lipids by SAXS experiment [22], also comparable results were obtained before in murine skin [21]. It has to be noticed that the formation of the LPP is strongly depending on the presence of long-chain ceramides as CER[EOH] or CER[EOS]. Especially CER[EOS], as the most lipophilic CER, is described as most essential for the SC barrier function. This correlates with results of studies on several diseases, where the skin protection shield is compromized due to reduced CER[EOS] levels [34-36]. The long-chain CER is discussed to be indispensable even for the body's water retention [35].

The other way around, Kessner and co-workers found out that LPP formation in CER[EOS] bulk phase requires high humidity [18]. Moreover, recent neutron diffraction studies were able to describe the LPP structure in SC lipid model membranes under high humidity and

determined the position of certain lipids by deuterium labeling [37-39]. These were the first experiments which revealed closer insights into the arrangement of lipids within the LPP. So further questions relating to the LPP and its coherence to the SC barrier property came up.

For example, the possibility to disturb the highly ordered structure temporarily and repairably in favor of higher drug penetration rates. For therapeutic or cosmetic reasons, it is desired to overcome the barrier properties and increase the influx through the skin. It was established that lipophilic penetration enhancers such as oleic acid (OA) or isopropyl myristate (IPM) displayed disordering effects on the rigid SC lipid membranes and are well approved in different cutaneous formulations [40-43]. The liquid wax isopropyl myristate (IPM) is known to increase the penetration rate of topically applied pharmaceuticals [44, 45]. Although a lipophilic molecule, IPM features a small polar part at the ester group. It does not provide a clear head-to-tail polarity, which is profitable for its interaction with the membranes [46, 47]. Possibly, IPM is able to partially dissolve the lipids of a SC intercellular membrane [48, 49]. WAXS and SAXS experiments localized the ester group of the enhancer in the polar membrane region and the alkyl chain pointing towards the unit cell center [50] compared to Engelbrecht et al., who additionally described a complete incoorperation of IPM using neutron diffraction [51].

In a first neutron diffraction study we tried to answer the question whether IPM could manipulate the assembling process of a SC lipid model membrane containing a modified methyl branched CER[EOS] (23 wt.%), CER[AP]-C18 (10 wt.%), cholesterol (CHOL) (33 wt.%) and behenic acid (BA) (33 wt.%), a system which had displayed a coexistence of SPP and LPP before [39]. Neutron diffraction is a versatile technique and offers a wide range of advantages for the investigation of SC lipid models compared to X-ray diffraction, in particular due to the varying coherent scattering lengths for the isotopes deuterium (^{2}H) and hydrogen (^{1}H) [52-55]. Applying deuterium labelled lipids within the model membranes, their positions and interactions on a molecular level are determinable, as performed in numerous works before [56-59].

Furthermore, we investigated the thermotropic phase behavior of the before mentioned SC lipid mixture. In order to accomplish these task, we heated it up to 50 °C and 70 °C in a second neutron diffraction experiment, followed by a final cooldown back to 32 °C. Former experiments with SC lipids showed phase transitions around that high temperatures [60] whereby even a recrystallization to a LPP was described [22].

The phase behavior of the SC lipid mixture was additionally proven with the established measuring method of ^{2}H NMR.

^{2}H solid-state NMR represents a powerful tool for investigating the structure and dynamics of lipid systems []. It also provides identification of the phase state of a certain component in the sample as well as quantification of phase proportions in the system [].

Our results show that these two techniques can go hand in hand and complement each other very well.

EXPERIMENTAL PART

Materials

CER[AP]-C18 ((N-(a-hydroxyoctadecanoyl)-phytosphingosine)) with a purity of 98 % was generously provided by Evonik Industries AG (Essen, Germany). CER[AP]-C18-*d3*, CER[EOS]-C30-C16-*d3* and IPM-*d3* were obtained by own chemical synthesis. While the IPM-*d3* synthesis was described earlier [51], the artificial CER[EOS]-C30-C16-br synthesis was specified in former works, where the product was characterized and analyzed by DSC and Fourier transform Raman spectroscopy studies to underline the comparability to the native CER[EOS]-C30-C18:2 [61]. The identity of the applied CERs was indicated by high resolution mass spectrometry. The detailed description of the deuterated CERs as well as perdeuterated IPM-*d27*, will be published soon. Cholesterol, behenic acid and the non-deuterated IPM were acquired from Sigma Aldrich GmbH (Steinheim, Germany) and used as received. Fig. (1) illustrates the chemical structures of the SC lipids, used for this experiment.

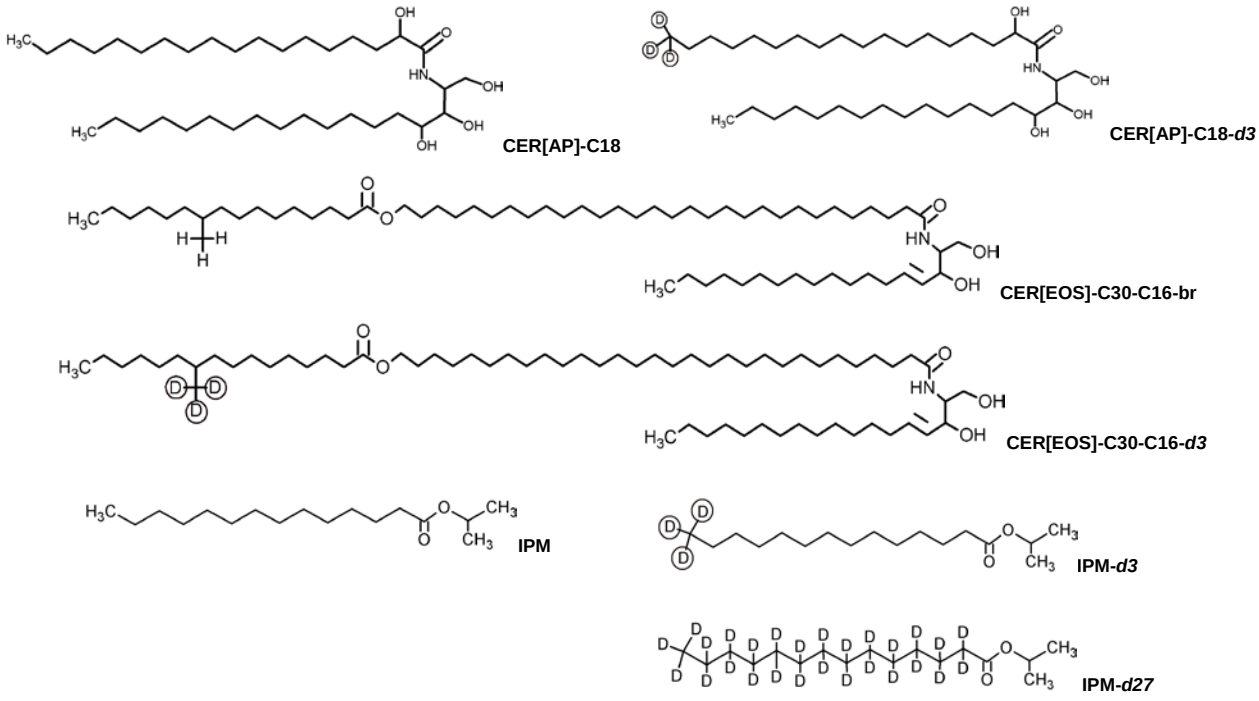

Fig. (1): Chemical structures of the applied ceramides and IPM next to their deuterated variations.

For the neutron diffraction experiments quartz slides with dimensions of 65 x 25 x 0.3 mm were optimal sample wafers due to their invisibility for neutrons. They were purchased from Saint-Gobain (Wiesbaden, Germany) as polished Spectrosil 2000. For the deposition of the lipids onto the quartz surface, a Hamilton pipette Model 725 RN SYR with a total volume of 250 µL was used.

Sample preparation

For the Neutron diffraction experiments, we prepared SC lipid model membranes, containing the partially deuterated ceramides [AP]-C18 and a modified long-chain ω-acyl CER[EOS], next to cholesterol (CHOL) and behenic acid (BA). A specifically deuterated IPM variation was added in a concentration of 10 %wt. relating to former comparable lipid mixtures [51]. The samples were prepared according to a known procedure to receive well oriented multilamellar lipid layers [62]. The lipids were dissolved separately in a chloroform/ methanol mixture (2:1; v/v) with a resulting concentration in the basic lipid solution of 10 mg/mL. The solvent mixture was chosen, due to its good solvent behavior for lipids and the fast required evaporation during the sample´s preparation. Both were bought from Merck (Darmstadt, Germany) in GC-grade. The next step involved their merging to the final lipid solutions with the desired ratios. Respectively, a volume of 1200 µL of the final lipid mixture was transmitted onto a quartz surface at a temperature of 70 °C. For a complete solvent removal, the samples were stored in a desiccator under room temperature and vacuum for 12 hours. The following annealing procedure allowed the lipid´s final assembling process during a heating-cooling cycle of at least four hours. During the heating period the samples were able to equilibrate under a water-saturated environment at 75 °C in an oven. At this temperature the lipid films became opaque due to their final arrangement in highly ordered multiple stacks. It was described before, that the state of order rises with the annealing process [63] and furthermore it is known, that a decreasing bilayer orientation results in a proportional lower number of structure factors [64]. This procedure is well-established in neutron scattering experiments based on higher peak intensities followed by a high benefit for the data analysis [64, 65]. In order to receive a LPP, the samples were stored under high humidity till the measurements. This procedure was described before [39].

In order to obtain the deuterium distribution of the system, four different samples were prepared (see Tbl. (1)).

SC lipid membrane model system	Designation	Ratio (wt.%)
I CER[AP]/CER[EOS]-br/CHOL/BA+ 10 % IPM	AP_EOS-br_IPM	10/23/33/33
II CER[AP]/CER[EOS]-br/CHOL/BA+ 10 % IPM-*d3*	AP_EOS-br_IPM-*d3*	10/23/33/33
III CER[AP]/CER[EOS]-*d3*/CHOL/BA+ 10 % IPM	AP_EOS-*d3*_IPM	10/23/33/33
IV CER[AP]-*d3*/CER[EOS]-br/CHOL/BA+ 10 % IPM-*d3*	AP-*d3*_EOS-br_IPM-*d3*	10/23/33/33

Tbl. (1): Composition of the investigated multilamellar membranes in the neutron diffraction studies. For determination of the deuterated label, the systems included one or two deuterated lipids, in italic.

For the performed ^{2}H NMR measurements, the sample either contained CER[AP18]-d_3, CER[EOS]-d_3 or IPM-d_{27} (see Tbl. (2)). For the sake of a better signal-to-noise ratio and the detection of an eventual effect of IPM on the model membrane we used 20 wt.% of the penetration enhancer in our ^{2}H NMR samples. For sample preparation, aliquots of each constituent were dissolved in chloroform/ methanol mixture (2:1; v/v). The solvent was subsequently evaporated using a rotary evaporator. The remaining lipid film was dissolved in cyclohexane and the sample was lyophilized overnight resulting in a powder, which was hydrated with 50 wt.% deuterium-depleted water. To prevent dehydration, samples were then filled into 4 mm MAS rotors and sealed for static ^{2}H NMR measurements. 24 h prior to spectra acquisition, samples were homogenized by freezing them in liquid nitrogen and heating them to 80°C. This treatment was repeated 10 times before incubating the samples at 22 °C. ^{2}H NMR spectra were acquired at three temperatures in the following order: 32 °C, 50 °C, 70 °C and 32 °C.

SC lipid model system	Designation	Ratio (wt.%)
I CER[AP]-*d3*/CER[EOS]-br/CHOL/BA+ 20 % IPM	AP-*d3*_EOS-br_IPM	10/23/33/33
II CER[AP]/CER[EOS]-*d3*/CHOL/BA+ 20 % IPM	AP_EOS-*d3*_IPM	10/23/33/33
III CER[AP]/CER[EOS]-br/CHOL/BA+ 20 % IPM-*d27*	AP_EOS-br_IPM-*d27*	10/23/33/33

Tbl. (2): Composition of the investigated lipid mixtures in the ^{2}H NMR studies.

Neutron diffraction experiments

The neutron diffraction experiments under skin temperature were performed by means of the instrument BIODIFF [66] at the Heinz Maier-Leibnitz Zentrum (MLZ), Garching, Germany. The diffractometer was originally designed for biological single crystal characterizations and is mostly used for protein structure determination with neutrons [67-70]. Here, for the first time, the instrument was used for the investigation of biological membrane structures, which required the installation of a new sample environment (see Fig. 2). Due to the variable pyrolytic graphite monochromator PG (002) in combination with a velocity selector ($\lambda/2$ filter) [71], a selected wavelength of 4.72 Å was realized. The detector was a cylindrical image plate (400 x 450 mm) [72], in the center of which the samples have been rotated (see Fig. (3)).

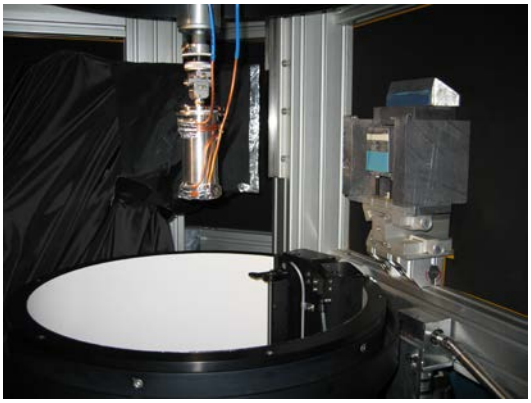

Fig. (2): New installed sample environment at BIODIFF, equipped with closable aluminum chambers (100 x 50 mm) and a Julabo F20 bath for temperature regulation.

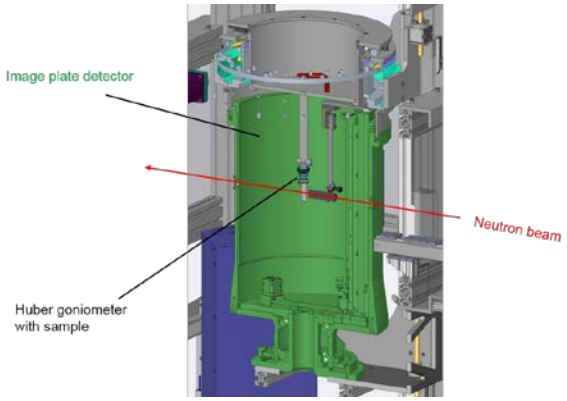

Fig. (3): Scheme of BIODIFF, modified to [73]. The sample was located in the middle of the cylindrical detector, fixed by a Huber goniometer.

Thus, the sample equilibration was executed at a constant temperature and well-defined relative humidity (RH) for 8 hours. Former experiments verified an equilibration time of 6-8 hours to achieve an optimized hydration level of SC lipid model membranes [23, 33, 61]. To compare to *in vivo* conditions, the samples were measured at the skin temperature of 32 °C. The samples were measured at 98 % RH, realized by a saturated solution of K_2SO_4 (Sigma-Aldrich, Steinheim, Germany) in D_2O/H_2O. The high humidity was chosen due to the higher chance of a LPP presence under CER[EOS] influence as described by Kessner et al. [18]. Each membrane was analyzed at three different D_2O contrasts (100/0, 50/50 and 8/92 % (v/v)) in order to compare the neutron scattering length density (NSLD) between water and lipids and to determine the SF´s phase signs.

At BIODIFF, the measurements for the first to third Bragg peak order included sample rotation of an ω-range from 0-21°, meaning a *2θ* angle from 0 to 42° within one hour (21° ω /h). One scan was repeated five times for better statistics. For the fourth and fifth Bragg peak order a scan with an ω-range from 9-21°, meaning a *2θ* angle from 18 to 42° in one hour (12°ω /h), was performed twice to get a more defined signal-to-noise ratio. Starting at 21 *2θ*, the determined intensities were additionally expanded by footprint correction to compensate the sample´s rotation beyond the beam. Moreover the different rotation velocities were relativized to 21° ω /h dividing the fourth and fifth order intensities by 1.75. Additionally, a background pattern was recorded.

The neutron diffraction experiments, which were focused on the thermotropic phase behavior of the SC lipid model membranes, were performed at the V1 Membrane Diffractometer at the cold source reactor of Helmholtz-Zentrum für Materialien und Energie (HZB, Berlin, Germany). The applied wavelength was 4.567 Å and the distance between sample and two-dimensional position-sensitive ^{3}He detector (area: 256 x 256 mm^2, spatial resolution: 2 x 2 mm^2) was 1025.7 mm. The one-dimensional diffraction experiment was performed by a reflection setup , which is described in detail elsewhere [31].

First of all, the samples were measured at 8 % D_2O and 98 % RH at skin temperature to compare the results to those received at BIODIFF. Here, the comparability between the neutron diffraction instruments was given. At 98 % RH the samples were heated up to 50 °C, 70 °C and cooled down to 32 °C. Here, only the changes of the first Bragg peak order were obtained during the heating periods. For the thermotropic phase behavior study, only 8 % D_2O was applied, since the scattering length of water is zero at this point [74, 75], hence it is not influencing the achieved data. Additionally, a scan with a clean quartz wafer in an empty can was performed to obtain the coherent and incoherent background level.

The scattering process in neutron diffraction studies is primarily described by Bragg´s law, $n\,\lambda = 2d \cdot \sin\theta$ where n is the diffraction order, d represents the spacing between the lattice planes of the lipid membranes and θ is the angle between the incident beam and the planes. Moreover, the change of the neutron´s momentum is demonstrated by the scattering vector Q. In detail, the incident neutron beam, described by $\overrightarrow{k_i}$, is scattered at the sample to the final wave vector $\overrightarrow{k_f}$ resulting in the scattering vector Q with $Q = k_f - k_i$. The scattering angle between $\overrightarrow{k_i}$, and $\overrightarrow{k_f}$ is $2\,\theta$. Due to $\left|\vec{k}\right| = \frac{2\,\pi}{\lambda}$, the final consolidation to the scattering context is possible with

$$Q = \frac{4\,\pi}{\lambda}\,\sin\theta \qquad \textbf{Equ. (1)}$$

The detectors registered the intensity I of the scattered neutrons as a function of the scattering angle$2\,\theta$. From the position of a series of equidistant peaks in the diffraction pattern, the periodicity (*d* or *d*- spacing) of the lamellar phases, was calculated using

$$d = \frac{2\,n\,\pi}{Q_n} \qquad \textbf{Equ. (2)}$$

The peak positions and intensities were determined by fitting Gaussian functions using the software package IGOR Pro Version 6.34A (WaveMetrics Inc., Portland, OR, USA). Thereby, the particular analysis of the integrated peak intensity I_h of the h^{th} order was performed [76]. Further, using I_h, the absolute values of their correlating structure factors F_h were calculated by $F_h = \sqrt{h \cdot A_h \cdot I_h}$ with A_h as absorption correction and h as Lorentz factor, which is related to the data collection geometry [77]. To infer conclusions about the nanoscaled membrane structure from the data, neutron scattering length density (NSLD) profiles $\rho_s(x)$ were calculated using Fourier transformation of the structure factors F_h according to [78]:

$$\rho_s(x) = a + b\,\frac{2}{d}\sum_{h=1}^{h_{max}} F_h\,cos\left(\frac{2\pi h x}{d}\right) \qquad \textbf{Equ. (3)}$$

where a and b represent unknown coefficients for relative normalization of $\rho_s(x)$, h the diffraction order with the associated structure factor F_h and *d* describes the lamellar repeat distance. The determination of the phase factor F_h was realized by contrast variation, which assumes "+" or "-" for centrosymmetric bilayers [64, 76] as the lamellar lipid phases are supposed to be organized. For this purpose, all samples were measured at least at three different D_2O/H_2O ratios, which provided a linear correlation between the $|F_h|$ value and D_2O content.

The final localization of the labelled group is possible due to the different coherent scattering length of neutrons for the isotopes hydrogen ^1H (b_{coh} = – 0.374 x 10^{-12} cm) and deuterium ^2H (*d*) (b_{coh} = +0.667 x 10^{-12} cm) [79]. Accordingly, the structure factors of the deuterated sample F_{h_deut} as well as the corresponding factors F_{h_prot} from the protonated sample were determined and used for the Fourier transformation. By the calculation of the difference density $\rho_{diff}(x) = \rho_{deut}(x) - \rho_{prot}(x)$, with ρ_{deut} as the NSLD of the partially deuterated sample and $\rho_{prot}(x)$ as the NSLD of the protonated sample, the position of the deuterated label within the lipid unit cell is visible by the resulting maxima in $\rho_{diff}(x)$.

^{2}H NMR experiment

All NMR spectra were acquired at a Bruker Avance 750 WB NMR spectrometer (Bruker BioSpin, Rheinstetten, Germany) using a deuterium resonance frequency of 115.1 MHz and a spectral width of ± 250 kHz. In the probe, a 5 mm solenoid coil was used. Measurements were conducted applying quadrature phase detection and a phase-cycled quadrupolar echo sequence with two 2-2.3 µs π/2 pulses separated by a 30 µs delay. The delay between two scans was 50 s. Samples were measured at temperatures of 32 °C, 50 °C, 70 °C and then again at 32 °C since previous studies showed that phase transitions were reversible but feature hysteresis [80]. For further processing of the acquired spectra a self-written Mathcad (MathSoft, Cambridge, MA) script [81] and NMR WEBLAB [82] were used.

RESULTS AND DISCUSSION

Characterization of the received single phase system by neutron diffractometer BIODIFF

For all samples, an ordered single phase system with five lamellar orders was obtained next to the crystalline CHOL peak (see Fig. (4)). Due to the positions of the equidistant peaks, a d-spacing of about 48 Å was calculated. The surplus percentage of CHOL, which could not be integrated into the membranes, is visible as separated crystalline cholesterol peak at an angle of 8.0°2θ. But its presence is not affecting the *d*-spacing of the lamellar structures [83].

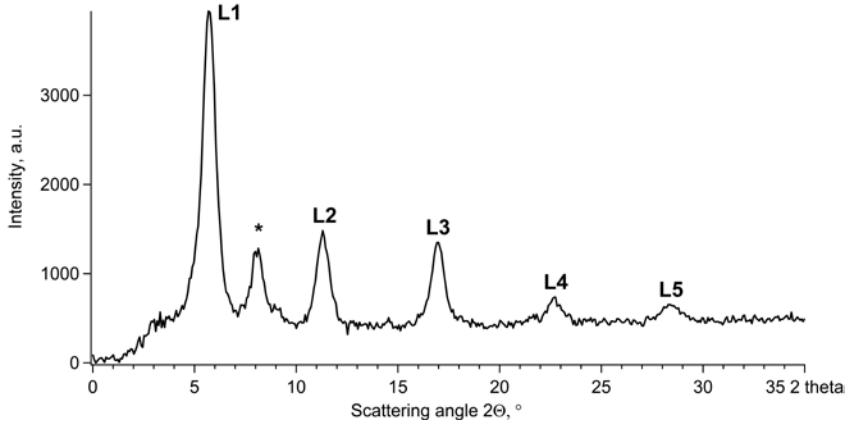

Fig. (2): The Bragg peak pattern of sample I, measured under 100 % D_2O contrast, 98 % RH and 32 °C. The described background subtraction was performed. The peak intensities are plotted against the scattering angle 2 θ. Next to the crystalline CHOL peak (*), the diffraction orders are given (L1-L5).

Referring to the described data treatment, the structure factors (SF) were received. Plotted against their corresponding D_2O contrast (see Fig. 5), the desired linearity was almost obtained. As described before, the phase signs for the systems are "+" or "-", meaning for the 1st to the 5th order (L, *h*) "- + - + -". Based on the decreasing peak intensity with rising number of order, the SFs are getting smaller from 1st to 5th order.

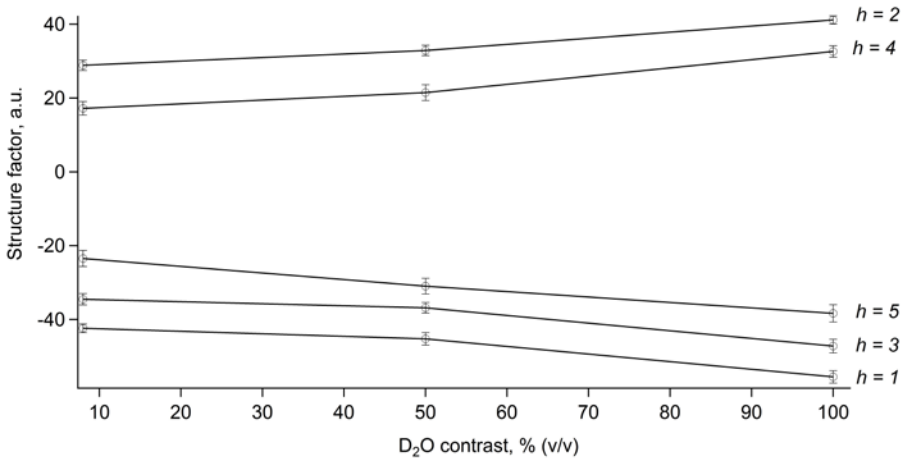

Fig. (3): Structure factors linearity of sample I. The lamellar orders are marked with *h* and the corresponding error bars. Thereby, the odd-numbered orders have a negative gain, due to their phase sign.

By Fourier transformation of the received SF, the NSLD profiles $\rho_s(x)$ at all three D_2O contrasts for the reference sample were received (see Fig. 6).

All NSLD profiles $\rho_s(x)$ show distinct maxima at the right and left border of the diagram, meaning a high atom density with several positive scattering length densities (SLD) in that area. This is interpreted as the position of the polar head groups. Additionally, the water distribution was calculated as difference of the several NSLD profile 100 % D_2O and 8 % D_2O. Hence, water is only located in a small amount at the polar head group region and not positioned besides the alkyl chains.

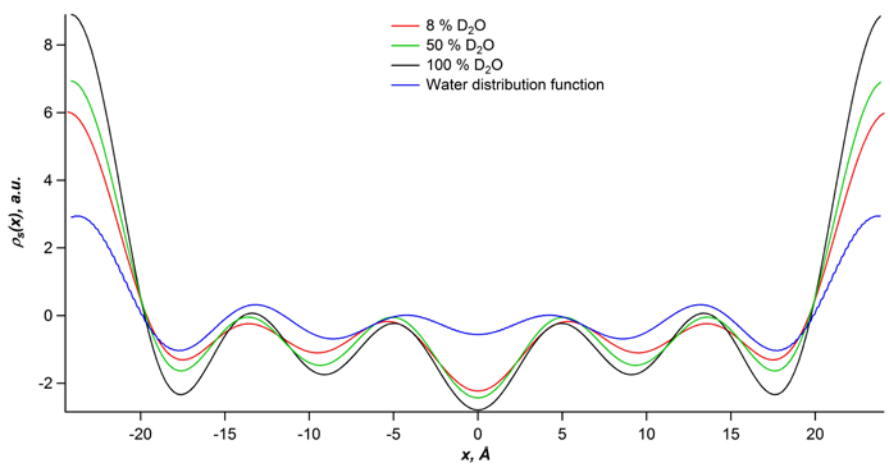

Fig. (4): The NSLD profile for sample I, received under 98 % RH and the skin temperature of 32 °C. The SL distributions of all three D_2O contents are presented, next to the water distribution, plotted against the unit cell scale in Å.

As declared in the theoretical part, repeat distances belonging to the SPP are described to be around 60 Å. With a d-spacing of about 48 Å, no such high numbers were reached. That is reasoned in the membrane compositions themselves, as they were composed of more complex lipid mixtures including several ceramide subclasses and fatty acids with longer alkyl chain length [58, 84]. Here, only four SC lipids were chosen, in order to get closer insights into the membrane assembling process with a more detailed comprehension for the structures and

lipid interactions. So, a lower d-spacing was accepted and even presented in former experiments [30, 33, 61], as it is scientifically approved.

At least, the lamellar spacing of 48 Å meant that the applied CER[EOS]-br did not induce the formation of a LPP unit cell. In an earlier experiment on the SC lipid system without penetration accelerator IPM, a multiphase system was obtained [39]. There, one of the three phases showed a bilayer spacing of 48 Å and with 7 lamellar orders a highly ordered system. A second phase formed a LPP with a d-spacing of about 114 Å [39].
Compared to the SC lipid model membrane without IPM, the smaller number of lamellar order as well as the formation of a single short-periodicity phase next to the absence of a LPP are interpreted as resulting effects of the applied accelerator.

Localization of the deuterated labels inside the SC lipid model membranes

To localize the deuterium label within the SC lipid model membranes, the normalized SFs were used. The measurements were performed under conditions of 8 % D_2O, 98 % RH and 32 °C. After Fourier transformation, the NSLD profile of the protonated control sample was subtracted from the NSLD profile of the deuterated sample. The lipophilic penetration enhancer IPM as well as the long-chain CER[EOS]-br were not detected within the received SPP (see Supplemental Material).
Sample II and IV were measured to determine only the position of CER[AP]. As mentioned above, sample IV included CER[AP]-*d3*, next to IPM-*d3*. The NSLD profiles of sample II and IV were compared to each other, as Fig. (7) presents.

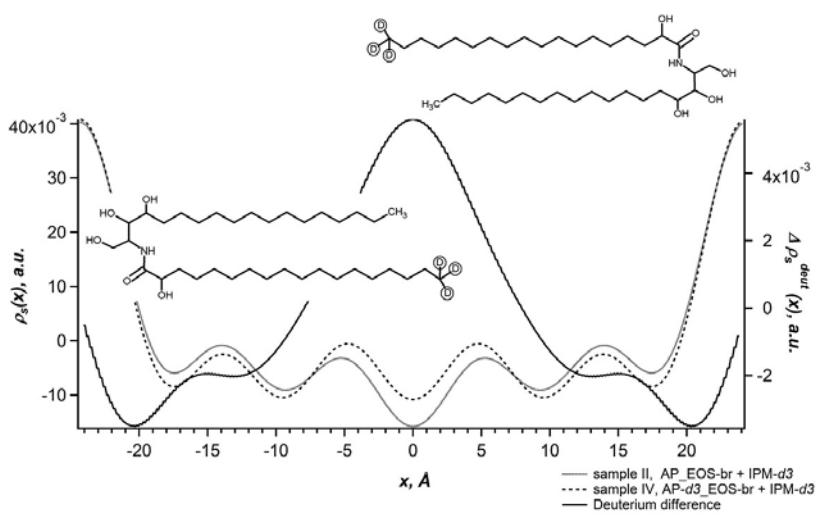

Fig. (7): The NSLD profiles of sample II (grey line) and IV (dotted line), received under 8 % D_2O, 98 % RH and 32 °C. Additionally, their difference is plotted (black line), with the outcome of the deuterium position of CER[AP] within the membrane.

Due to the difference of both samples, the deuterium labels were determined between -7.5 and 7.5 Å in the bilayer center, with a significant maximum at ± 0 Å (see Fig. (7)). The amid bound C18 fatty acid of CER[AP] had a chain length of 22.86 Å in its all-*trans*

conformation, based onto a length of 1.27 Å per C-C bond [85, 86].The arrangement of two CER[AP] molecules opposite each other would mean a total spacing of 45.72 Å for the fatty acid chains, respectively. Including the spacing of the polar head groups, the proposed bilayer arrangement is possible.

Furthermore, we supposed CER[AP]-*d3* in its hairpin conformation, whereby the polar head groups were positioned at the bilayer edges and the non-polar alkyl chains arranged towards the bilayer center. The interdigitation of CER[AP] alkyl chain ends was assumed before for a SPP of 48 Å [32, 33]. We were able to confirm that idea, as the broad deuterium maximum in the bilayer center indicates the high presence of deuterium in that area. Together with the molecule chain lengths, the interdigitation was proven. Comparable results were described before for CER[NS]-C24 in a SPP of about 54 Å as well [84]. As far as the authors know, this is the first study, which localized CER[AP]-C18 in a single short-periodicity phase in a SC lipid model membrane.

Unfortunately, there was no insight into the actual ceramide conformation at this point. Therefore, further experiments with different positions of the deuteration are planned.

Thermotropic phase behavior – a neutron diffraction study

For closer insight into the SC lipid model membrane properties, the thermotropic phase behavior was a further point of interest. First, we have to underline, that there is no correlation of this experimental part to natural occurring SC, as no temperatures in that dimensions are realistic. But for an extensive understanding of the applied SC lipid model and its characteristics, the focus on changes under the impact of temperature was relevant, too. Furthermore, the stability of the lipid system after the sample preparation was a point of interest, as the possibility of a LPP appearance was given under high humidity and temperatures. For the investigation of the phase behavior the lipid model system containing IPM-*d3* was chosen. Here, the single acting of the penetration accelerator under higher temperatures took center stage. The sample was heated from 32 °C to 50 °C under high humidity, as Fig. (8) presents. The Bragg peak pattern of the first lamellar order at 0.132 $Å^{-1}$ showed neither changes in position nor intensity. The SC lipid model membrane was very stable in its multilayer structure during that first heating period. Only the peak position of crystallized cholesterol shifted slightly from 0.185 to 0.182 $Å^{-1}$, with no further meaning for the data discussion. But reaching 55 °C, an additional peak appeared at 0.151 $Å^{-1}$ and simultaneously the intensities of the first Bragg peak order and the CHOL peak decreased. With higher temperatures, the intensity of the additional peak increased enormous. At 60 °C, the first Bragg peak order started to increase, whereby the crystalline cholesterol was integrated completely into the SC lipid membranes, as the corresponding signal disappeared. Both remaining peaks reached their maximum intensity at 70 °C. Due to the rising energy

inside the lipid model membranes, at 55 °C a phase transition started and phase separation occurred. A new organization of the present lipids with a more stable arrangement was reached as the higher peak intensities revealed.

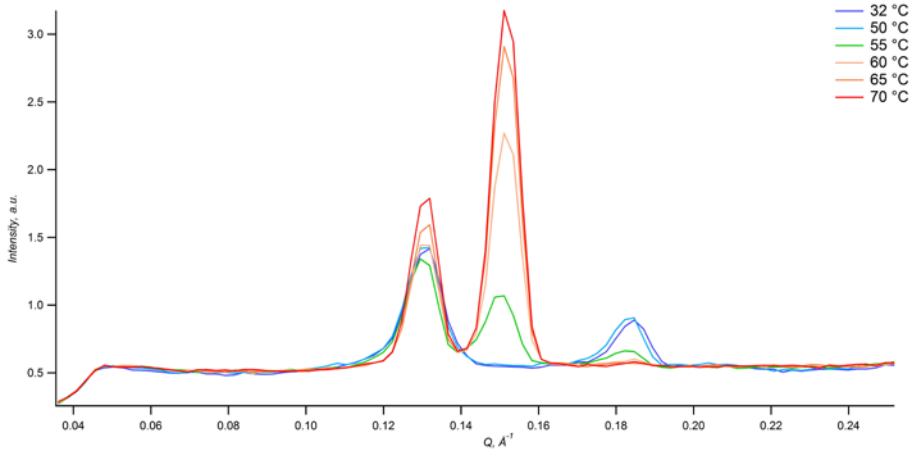

Fig. (8): Rocking curve of sample II, AP_EOS-br + IPM-*d3* during the heating period from 32 °C to 70 °C, received under 8 % D_2O and 98 % RH. Here, the detector position was optimized for the first lamellar order scan at 0.132 $Å^{-1}$ (L1).

Afterwards the phase behavior of the presented SC lipid model membrane under a cooling procedure was observed (see Fig. 9). With decreasing temperature, a lipid reorganization started. At 65 °C a third phase appeared with three equidistant Bragg peak orders at 0.062 $Å^{-1}$ (L1), 0.124 $Å^{-1}$ (L2) and as a shoulder of the high crystalline CHOL peak at 0.186 $Å^{-1}$ (L3). Using the positions of the present three lamellar order and a wavelength λ of 4.567 Å, a d-spacing of 100.76 Å was calculated. Compared to the SC lipid model membrane without IPM, where a LPP with about 114 Å was observed [39], we had distinct evidence for the appearance of a LPP here, too. With further decreasing temperature, the peak intensities of the LPP became smaller, too. At 55 °C the 1st and 2nd lamellar orders were only visible as small signals. Simultaneously, the peaks shifted towards smaller *Q* values, meaning a final d-spacing of 111.45 Å at 32 °C. Although a LPP appeared, this phenomenon was highly associated to the temperature. On one hand, the applied CER[EOS]-br was able to support the formation of a LPP but on the other hand the phase transition during the cooling procedure reduced its stability noticeably. These results gave more material for the debate of the presence and stability of a LPP in SC lipid model membranes.

Even the peak intensity of excessive CHOL at 0.183 $Å^{-1}$ changed measurably, meaning its partial incorporation and final recrystallization at 32 °C. Moreover, the intensity of the peak at 0.151 $Å^{-1}$, which appeared during the heating period, fluctuated highly during the cool down. At 65 °C, another peak appeared at 0.168 $Å^{-1}$ with its maximal intensity at 55 °C. At 32 °C the peak reached its final position at 0.160 $Å^{-1}$. Especially full θ-2θ scans will be necessary to gain

further knowledge about the lipids and possible phases they form. From the actual point of view, we can interpret the extra peaks as markers for a multifactorial lipid rearrangement.

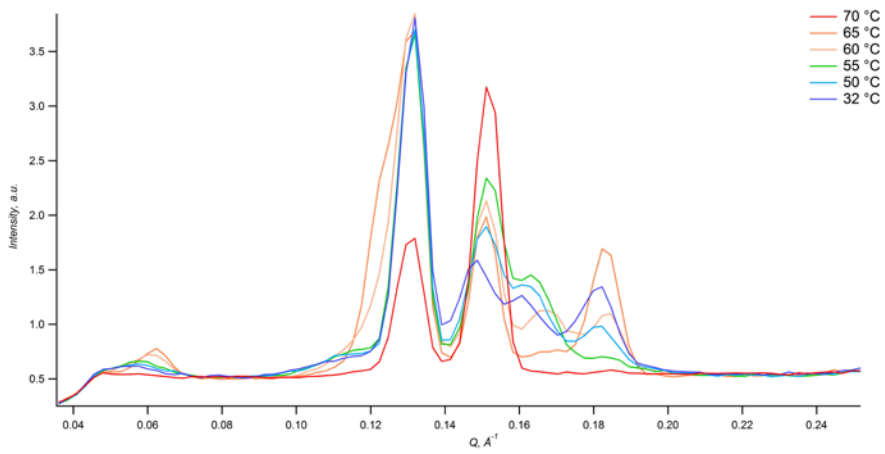

Fig. (9): Rocking curve of sample II, AP_EOS-br + IPM-*d3* during the cooling period from 70 °C to 32 °C, received under 8 % D_2O and 98 % RH. Here, the detector position was optimized for the first lamellar order scan at 0.132 Å^{-1} (L1).

Thermotropic phase behavior- a ^{2}H-NMR study

While deuterated methyl groups represent a great tool to localize these molecular segments of lipids in SC models using neutron diffraction, they can also be employed in ^{2}H NMR measurements. A number of successful ^{2}H NMR studies have helped understanding the structure and phase composition of various SC model systems. Typically, perdeuterated free fatty acids [23, 87] or ceramide species [88-90] have been employed to understand the thermotropic phase behavior of complex SC mixtures, but meaningful insights have also been derived from specifically labeled cholesterol [23, 91] in the mixture. Specifically methyl-deuterated probes in ceramides are less suited to study the phase composition of these molecules, but represent very good probes to investigate the molecular dynamics of the ceramide acyl chains. Methyl groups undergo 3-site hopping motions, which scale the quadrupolar couplings of an otherwise rigid CH_3 group to 41.75 kHz, which is 1/3 of its maximal value. Thus, methyl groups can be detected with relatively high sensitivity and alterations of the detected line shape from the classic Pake doublet are indicative of motions in a broad correlation time window up to the intermediate microsecond range [92].

In the model system, we have switched the ^{2}H label either between the terminal methyl group of CER[AP] or CER[EOS]-br, thus obtaining information about the dynamics of these molecular segments. In phospholipid membranes, the terminal methyl groups are highly disordered and undergo large amplitude motions yielding molecular order parameters smaller than 0.02. However, in SC models even the terminal methyl groups are more ordered. Fig. 10 shows the ^{2}H NMR spectra of CER[AP]-*d*3_CER[EOS]-br_CHOL_BA + 20 wt.% IPM (left), CER[AP]_CER[EOS]-*d3*_CHOL_BA + 20 wt.% IPM and CER[AP]_CER[EOS]-br_CHOL_BA + 20 wt.% IPM-*d27* (right) at three temperatures. There is no indication of the presence of a rigid orthorhombic phase, which would have manifested by

a Pake spectrum with a quadrupolar splitting of around 40 kHz. In contrast, even at physiological skin temperature, both ceramide species show spectra that are indicative of motions that can be described by a two-site hop model [93]. In this model, the -C-CH_3 bond is assumed to hop between two sites with a hopping angle of 120°. This hopping appears to occur at a rate, which is faster than the inverse of the quadrupolar interaction strength, which is in the range of microseconds.[2]

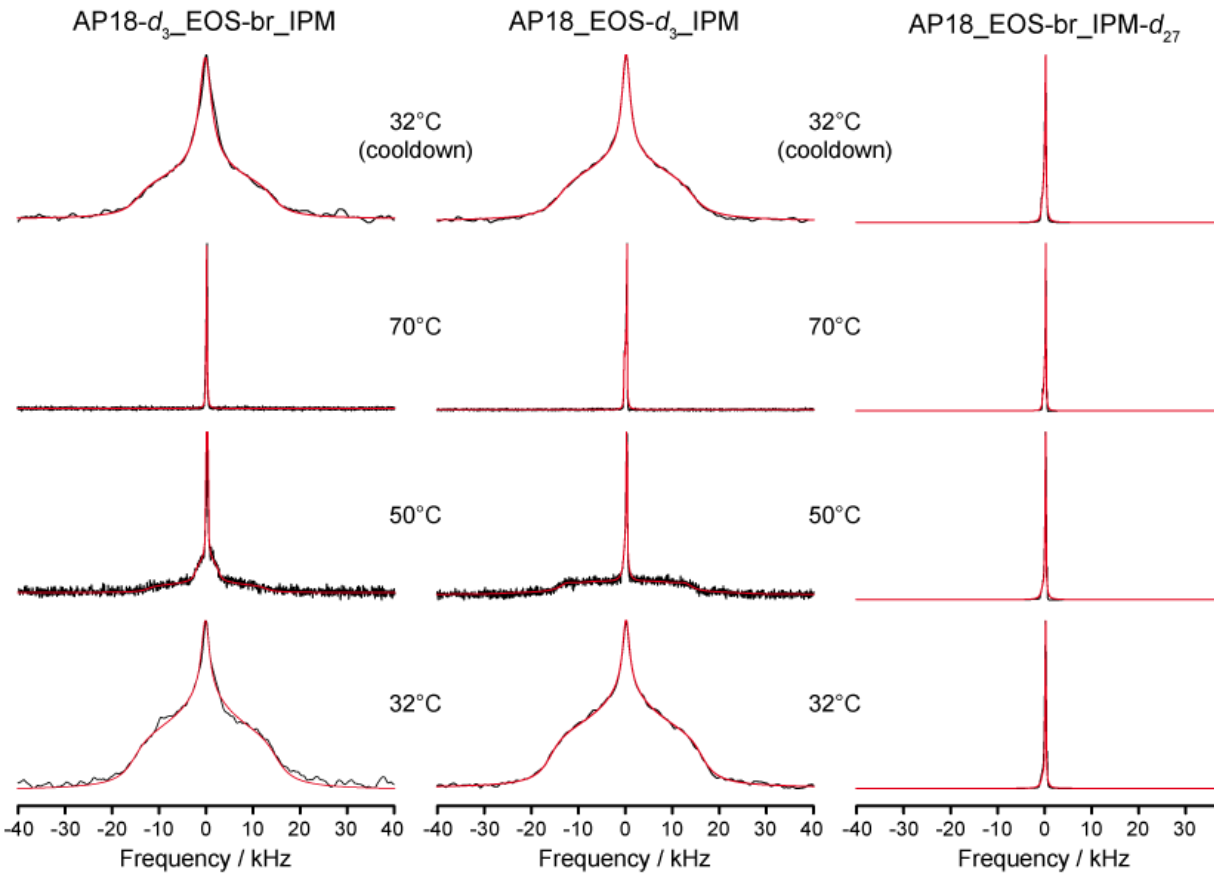

Fig. (10): ^{2}H NMR spectra of the mixture AP_EOS-br_IPM at given temperatures at a hydration level of 50 wt.%. The left column shows the spectra of the mixture containing specifically deuterated AP-d_3, the middle column depicts spectra of the EOS-d_3 and the right column displays the spectra of IPM-d_{27}. ^{2}H NMR spectra were acquired using a repetition time of 50 s. The red lines represent the numerically simulated fits of the acquired spectra (black lines).

The simulations of the NMR spectra require input of the motionally averaged quadrupolar coupling. As mentioned above, this value is 41.75 kHz for a rotating methyl group, but can be further averaged by motions of the chain of the ceramides. This is typically expressed by an order parameter that defines the motional amplitude of a specific bond vector of a given protein [94-96]. With these considerations, we can discuss the motions of the methyl groups of CER[AP]-C18 and CER[EOS]-br, respectively. At 32 °C, both groups undergo the aforementioned two-site hopping but in addition, the bond vectors fluctuate expressed by an order parameter of 0.72 for CER[AP]-C18 and 0.77 for CER[EOS]-br. At elevated temperature

of 50 °C, the spectra of both ceramide species become much narrower indicating large amplitude and isotropic motions, the latter of which dominate the mixture at 70 °C. After cooling both samples down again to skin temperature spectra show that the two-site hopping is reproducible. Nevertheless, its contribution to spectral intensity is less than before heating to 50°C. This can be interpreted as a hysteresis behavior which has already been reported for ceramide (bovine brain ceramide, Type III) containing SC model systems [80].

Very surprisingly, IPM showed isotropic ^{2}H NMR spectra at all temperatures, which means that the IPM is always highly mobile and may be organized in a structure with highly curved surfaces such as a micellar or cubic phase.

CONCLUSION

We investigated how the penetration enhancer IPM influences the structure of stratum corneum lipid model membranes containing CER[AP], CER[EOS]-br, behenic acid, and cholesterol. Using neutron diffraction, we found that our model system featured a single SPP with a lamellar repeat distance of about 48 Å. Thereby five Bragg peaks gave a good lamellar order. These results are in contrast to a former study, where a highly ordered multiphase system with coexisting SPP and LPP was reported [39]. It can thus be attributed to the disordering effect of IPM on SC models. Even the permanent impact of high humidity and the presence of the long-chain ceramide [EOS]-br did not generate a LPP at skin temperature.

In our study, the long chain CER[EOS]-*d3* variation was not even detected in the SPP which revises an earlier model proposing the long chain ceramide's integration into a 48 Å SPP [61]. But we were also able to localize the methyl groups of CER[AP]-C18 and from that concluded its position within the lateral organization of the model membrane. Our data confirmed former ideas of the CER[AP] position within comparable lipid mixtures [32, 33].

Although we observed a defined effect of the penetration accelerator IPM to the applied SC lipid model membrane in the neutron diffraction studies, we were not able to localize it inside the bilayer structure. A reason therefore was found in the ^{2}H NMR studies, which revealed IPM in an isotropic phase state at all temperatures. This could mean that IPM wasn't incorporated into the model membrane at all, which would be very surprising since former neutron diffraction studies described several IPM positions in SC lipid model membranes [51].

The neutron scattering studies of the thermotropic phase behavior figured out a significant phase transition above 55 °C. Simultaneously, the ^{2}H NMR study revealed a phase transition even between 32 °C and 50 °C. Furthermore, from the ^{2}H NMR experiment we can consider that the ratio of ordered lipids was only 5 % at 70 °C.

During the cool down procedure, a hysteresis effect of the lipids was determined. We were able to observe several phase transitions meaning the appearance of an additional phase and peaks. Here, especially CER[EOS]-br was involved as the first three lamellar Bragg peak orders of a LPP with a repeat distance of about 100 Å were visible. High humidity as well as high temperatures during the measurement induced a LPP using CER[EOS]-br.

Summarizing we were able to observe a disordering effect of IPM to a well-known SC lipid model membrane. As the penetration enhancer was not integrated within the membranes, the exactly mode of action will be focused in further studies.

ACKNOWLDEGEMENTS

This work is based upon experiments performed at the BIODIFF instrument operated by JCNS and FRM II at the Heinz Maier-Leibnitz Zentrum (MLZ), Garching, Germany. The authors gratefully acknowledge the financial support provided by JCNS to perform the neutron scattering measurements at the Heinz Maier-Leibnitz Zentrum (MLZ), Garching, Germany. Furthermore, the authors would like to thank the Helmholtz- Zentrum Berlin für Materialien und Energie (Berlin, Germany) for the allocation of neutron radiation beamtime for the thermotropic phase behavior study and the financial support. Moreover, Evonik Industries AG (Essen, Germany) is gratefully acknowledged for the generous donation of CER[AP]-C18.

SUPPLEMENTAL MATERIAL

Structure factors of sample I

Tbl. (a) presents the absolute SF and corresponding errors of the protonated control sample I at all D_2O contrasts.

Contrast	L1	L2	L3	L4	L5
8 %	-42.3728 ± 1.1822	28.8535 ± 1.3907	-34.5246 ± 1.5398	17.1992 ± 1.8274	-23.4822 ± 2.1885
50 %	-45.2581 ± 1.5772	32.8742 ± 1.4136	-36.8490 ± 1.4832	21.4707 ± 2.1417	-30.9876 ± 2.3706
100 %	-55.5356 ± 1.7049	41.1337 ± 1.1168	-47.2109 ± 1.8578	32.5949 ± 1.5597	-38.3378 ± 2.3559

Absence of IPM-d3 in SPP

For the position determination of the penetration accelerator, sample II included the *d3*-labeled IPM. Furthermore, the presence of IPM-*d3* was tested due to sample IV, where additionally CER[AP]-*d3* was incorporated. Fig. (a) and Fig. (b) included the corresponding NSLD profiles next to the deuterium differences. The deuterium difference curve of single IPM-*d3* in Fig. (a) indicated two maxima at ± 18 Å and a small peak at the membrane center. Based onto the minimal central peak in negative dimensions for the NSLD, no position for a deuteration was located here. More interesting are the maxima of the difference curve at ± 18 Å. Here, deuterium labels could be present but they were located at the changeover from the polar to the non-polar area of the bilayer. So they were results of truncation errors, which we could review by Fig. (b). There, next to a significant central peak (corresponding to CER[AP]-C18-*d3*), only very small and broad signals were found around ± 18 Å. Together with the reasonable suspicion of truncation errors in Fig. (a), the very parallel progress of both NSLD profiles at the slopes in Fig. (b) admitted the conclusion of IPM-*d3* absence in the investigated SC lipid model membrane system.

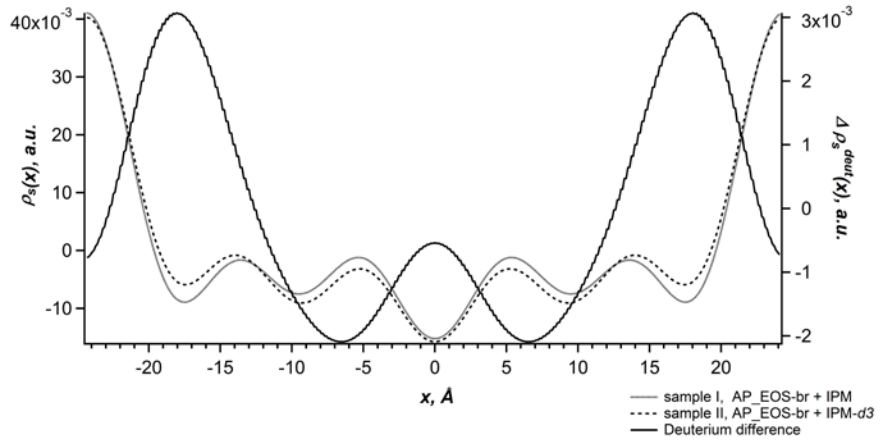

Fig. (a): The NSLD profiles of sample I (grey line) and II (dotted line), received under 8 % D_2O, 98 % RH and 32 °C. Next to them, their difference is plotted (black line), with the outcome of the deuterium positions of IPM within the membrane.

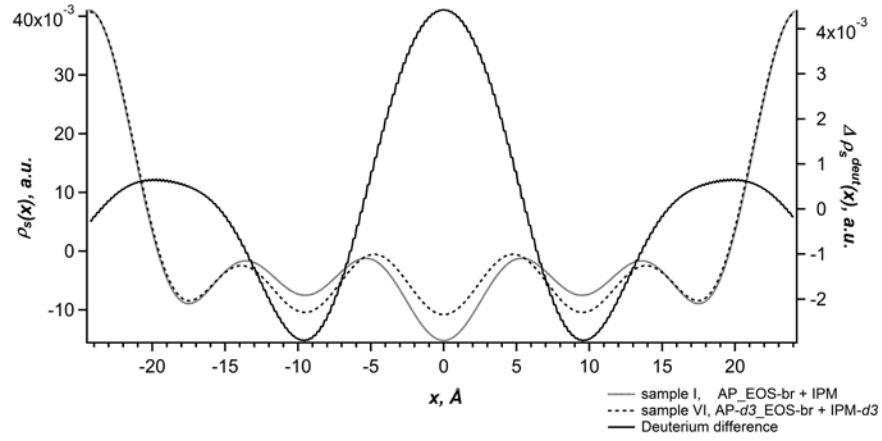

Fig. (b): The NSLD profiles of sample I (grey line) and IV (dotted line), received under 8 % D_2O, 98 % RH and 32 °C. Next to them, their difference is plotted (black line), with the outcome of the deuterium positions of IPM and CER[AP] within the membrane.

That was surprising, as former neutron scattering experiments with IPM-*d3* verified two possible position of the lipophilic penetration enhancer within a comparable SC lipid model membrane system, with absent CER[EOS]-br [51]. Especially the small head-to-tail-polarity of the molecule gave expectations about its presence within the lipophilic SC model membranes. Due to the hydrophobic match [97], the interaction of the IPM´s myristic acid with the behenic acid molecules could stabilize the lipids along each other. But as the performed ^{2}H NMR experiment revealed, the perdeuterated IPM was isotropic all the time and not integrated into the lipid membranes. So IPM was able to influence the lipids assembling process and their phase behavior without being present within the lamellar layers.

Absence of CER[EOS]-d3 in SPP

Sample III included the *d3*-labeled long-chain ω-acyl ceramide [EOS] species, to determine its position within the lipid membranes.

Although the preparation method was adapted from an earlier experiment [39], here no LPP formation was observed. So the question was, if the deuterated long-chain CER could be arranged within the short-periodicity phase as former experiments assumed [33, 56, 61]. The NSLD profiles of the protonated sample I and deuterated sample III were plotted in Fig. (c) next to their resulting deuterium difference.

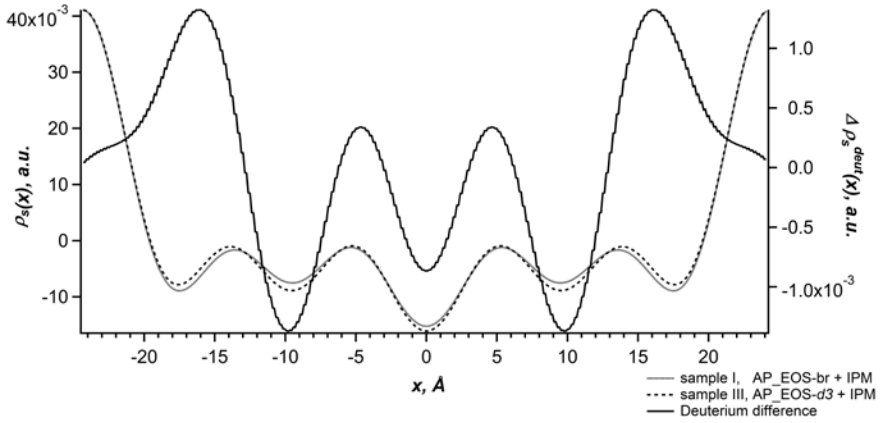

Fig. (c): The NSLD profiles of sample I (grey line) and III (dotted line), received under 8 % D_2O, 98 % RH and 32 °C. Additionally, their difference is plotted (black line), with no significant position of CER[EOS]-*d3* within the membrane.

The progress of the curves is nearly congruent and the differences were in the magnitude of truncation errors, especially at the maxima at ± 16 Å. Additionally, the minimum and maximum amplitude were in comparable dimensions. For a significant deuterium difference, the positive amplitude should be higher than the negative progress. So, the application of the partial deuterated CER[EOS]-*d3* gave no information about the position of the CER within the 48 Å phase. We assume, that the long-chain CER was not integrated into the short phase. Moreover the ceramide was not arranged within another oriented bilayer structure, as a single phase system was received. It seemed as its long and static structure inhibited the inclusion into short-periodicity phases. Compared to an earlier assumed model, where by molecular dynamics simulations the phase behavior of CER[EOS]-br was imagined [61], we are now able so revise this model.

LITERATURE

1. Wertz, P.W. and B. van den Bergh, *The physical, chemical and functional properties of lipids in the skin and other biological barriers.* Chem Phys Lipids, 1998. **91**(2): p. 85-96.
2. Scheuplin, R.J., *Permeability of the skin: A review of major concepts and some new developments.* The Journal of Investigative Dermatology, 1976. **67**(5): p. 672-676.
3. Elias, P.M., *Epidermal Lipids, Barrier Function and Desquamation.* The Journal of Investigative Dermatology, 1983. **80**(6): p. 44s-49s.
4. Yardley, H.J. and R. Summerly, *Lipid composition and metabolism in normal and diseased epidermis.* Pharmacology & Therapeutics, 1981. **13**(2): p. 383.
5. Gray, G.M., Yardley, H. J., *Different populations of pig epidermal cells: isolation and lipid composition.* Journal of Lipid Research, 1975. **16**(6): p. 441-447.
6. Coderch, L., et al., *Ceramides and skin function.* Am J Clin Dermatol, 2003. **4**(2): p. 107-29.
7. Wertz, P.W., van den Bergh, B., *The physical, chemical and functional properties of lipids in the skin and other biological barriers.* Chemistry ans Physics of Lipids, 1998. **91**(2): p. 85-96.
8. Masukawa, Y., Narita, H., Kitahara, T., Takema, Y., Kita, K., *Characterization of overall ceramide species in human Stratum corneum.* Journal of Lipid Research, 2008. **49**(7): p. 1466-1476.
9. van Smeden, J., Hoppel, L., van der Heijden, R., Hankemeier, T., Vreeken, R. J., Bouwstra, J. A., *LC/MS analysis of Stratum corneum lipids: Ceramide profiling and discovery.* Journal of Lipid Research, 2011. **52**(6): p. 1211-1221.
10. Rabionet, M., Gorgas, K., Sandhoff, R., *Ceramide synthesis in the epidermis.* Biochimica et Biophysica Acta, Molecular and Cell Biology of Lipids, 2014. **1841**(3): p. 422-434.
11. t´Kindt, R., Jorge, L., Dumont, E., Couturon, P., David, F., Sandra, P., Sandra, K., *Profiling and characterizing skin ceramides using reversed-phase liquid chromatography-quadrupole time-of-flight mass spectrometry.* Analytical Chemistry, 2012. **84**: p. 403-411.
12. Masukawa, Y., Narita, H., Sato, H., Naoe, A., Kondo, N., Sugai, Y., Oba, T., Homma, R., Ishikawa, J., Takagi, Y., Kitahara, T.,, *Comprehensive quantification of ceramide species in human stratum corneum.* Journal of Lipid Research, 2009. **50**: p. 1708-1719.
13. Liou, Y.-B., Sheu, M.-T., Liu, D.-Z., Lin, S.-Y., Ho, H.-O, *Quantitation of ceramides in nude mouse skin by normal-phase liquid chromatography and atmospheric pressure chemical ionization mass spectrometry.* Analytical Biochemistry, 2010. **401**: p. 107-113.
14. Sahle, F.F., Lange, S., Dobner, B., Wohlrab, J., Neubert, R. H. H., *Development and validation of LC/ESI-MS method for the detection and quantification of exogenous ceramide NP in stratum corneum and other layers of the skin.* Journal of Pharmaceutical and Biomedical Anlysis, 2012. **60**: p. 7-13.
15. Cho, H.J., Chung, B. Y., Lee, H. B., Kim, H. O., Park, Ch. W., Lee, Ch. H., *Quantitative study of stratum corneum ceramides contens in patients with senisitve skin.* Journal of Dermantology, 2012. **39**: p. 2012.
16. Park, S.Y., Kim, J. H., Cho, S. I., Kim, K. I.,Cho, H. J., Park, Ch. W., Lee, Ch.H., Kim, H. O., *Induction of a Hardening Phenomenon and Quantitative Changes of Ceramides in Stratum Corneum.* Annals of Dermatology, 2014. **26**(1): p. 35-42.
17. de Sousa Neto, D., Gorris, G., Bouwstra, J., *Effect of the ω-acylceramides on the lipid organization of stratum corneum model membranes evaluated by X-ray diffraction and FTIR studies.* Chemistry and Physics of Lipids, 2011. **164**: p. 184-195.
18. Kessner, D., Brezesinski, G., Funari, S. S., Dobner, B., Neubert, R. H. H., *Impact of long chain ω-acylceramides on the stratum corneum lipid nanostructure. Part 1 : Thermotropic phase behaviour of CER[EOS] and CER[EOP] studied using X-ray*

powder diffraction and FT-Raman spectroscopy. Chemistry and Physics of Lipids, 2010. **163**: p. 42-50.
19. Groen, D., Gooris, G. S., Bouwstra, J. A., *New Insights into the Stratum Corneum Lipid Organization by X-Ray Diffraction Analysis.* Biophysical Journal, 2009. **97**: p. 2242-2249.
20. Madison, K.C., Swartzendruber, D. C., Wertz, P.W., Downing, D. T., *Presence of intact intercellular lipid lammellae in the upper layers of the stratum corneum.* The Journal of Investigative Dermatology, 1987. **88**(6): p. 714-718.
21. White, S.H., Mirejovsky, D., King, G. I., *Structure of lamellar lipid domains and corneocyte envelopes of murine stratum corneum. An X-ray diffraction study.* Biochemistry, 1988. **27**: p. 3725-3732.
22. Bouwstra, J.A., Gooris, G. S., van der Spek, J. A., Bras, W., *Structural investigations of human stratum corneum by small-angle X-ray scattering.* Journal of Investigative Dermatology, 1991. **97**(6): p. 1005-1012.
23. Engelbrecht, T.N., Schroeter, A., Hauß, T., Demé, B., Scheidt, H. A., Huster, D., Neubert, R. H. H., *The impact of ceramides NP and AP on the nanostructure of stratum corneum lipid bilayer. Part I: neutron diffraction and ^{2}H NMR studies on multilamellar models based on ceramides with symmetric alkyl chain length distribution.* Soft Matter, 2012. **8**: p. 2599-2607.
24. de Jager, M.W., Gooris, G. S., Dolbnya, I. P., Bras, W., Ponec, M., Bouwstra, J. A., *The phase behaviour of skin lipid mixtures based on synthetic ceramides.* Chemistry and Physics of Lipids, 2003. **125**(2): p. 123-134.
25. Bouwstra, J.A., Gooris, G. S., Frank, E. R., Ponec, M., *Phase behaviour of stratum corneum lipid mixtures based on human ceramides: The role of natural and synthetic ceramide 1.* Journal of Investigative Dermatology, 2002. **118**(4): p. 606-617.
26. Kiselev, M.A., Ermakova, E. V., Gruzinov, A. Yu., Zabelin, A. V., *Formation of the long-periodicity phase in model membranes of the outermost layer of skin (Stratum corneum).* Crystallography Reports, 2014. **59**(1): p. 123-128.
27. Bouwstra, J.A., Gooris, G. S., Dubbelaar, F. E. R., Weerheim, A. M., IJzerman, A. P., Ponec, M., *Role of ceramide 1 in the molecular organization of the stratum corneum lipids.* Journal of Lipid Research, 1998. **39**(1): p. 186-196.
28. Bouwstra, J.A., Gooris, G. S., Dubbelaar, F. E. R., Ponec, M., *Phase behaviour of lipid mixtures based on human ceramides: coexistence of crystalline and liquid phases.* Journal of Lipid Research, 2001. **42**(11): p. 1759-1770.
29. McIntosh, T.J., Stewart, M. E., Downing, D. T., *X-ray diffraction analysis of isolated skin lipids: Reconstruction of intercellular lipid domains.* Biochemistry, 1996. **35**(12): p. 3649-3653.
30. Schroeter, A., *The role of ceramide (AP) for the structural assembly of stratum corneum lipid model membranes*, in *Institute of Pharmacy*. 2010, Martin Luther University Halle-Wittenberg: Halle.
31. Ruettinger, A., Kiselev, M. A., Hauss, T., Dante, S., Balagurov, A. M., Neubert, R. H. H., *Fatty acid interdigitation in stratum corneum model membranes: a neutron diffraction study.* European Journal of Dermatology: EJD, 2008. **37**(6): p. 759-771.
32. Schroeter , A., Kiselev, M.A., Hauß, T. Dante, S., Neubert, R.H.H., *Evidence of free fatty acid interdigitation in stratum conreum model membranes based in ceramide [AP] by deuterium labelling.* Biochimica et Biophysica Acta, 2009. **1788**(10): p. 2194-2203.
33. Schroeter , A., Kessner, D., Kiselev, M.A., Hauß, T. Dante, S., Neubert, R.H.H., *Basic nanostructure of stratum corneum lipid matrices based on ceramides [EOS] and [AP]: A neutron diffraction study.* Biophysical Journal, 2009. **97**: p. 1104-1114.
34. Di Nardo, A., Wertz, P., Giannetti, A., Seidenari, S., *Ceramide and cholesterol compostion of the skin of patients with atopic dermatitis.* Act dermato-venereologica, 1998. **78**(1): p. 27-30.
35. Motta, S., Monti, M., Sesana, S., Mellesi, L., Ghidoni, R., Caputo, R., *Abnormality of water barrier function in psoriasis. Role of ceramide fractions.* Archives of Dermatology, 1994. **130**(4): p. 452-456.

36. Motta, S., Monti, M., Sesana, S., Caputo, R., Carelli, S., Ghidoni, R., *Ceramide composition of the psoriatic scale.* Biochimica et Biophysica Acta, 1993. **1182**: p. 147-151.
37. Mojumdar, E.H., Gooris, G. S., Barlow, D. J., Lawrence, M. J., Demé, B., Bouwstra, J. A., *Skin Lipids: Localization of ceramide and fatty acid in the unit cell of the long periodicity phase.* Biophysical Journal, 2015.
38. Mojumdar, E.H., Gooris, G. S., Groen, D., Barlow, D. J., Lawrence, M. J., Demé, B., Bouwstra, J. A., *Stratum corneum lipid matrix: Localization of acyl ceramide and cholesterol in the unit cell of the long periodicity phase.* Biochimica et Biophysica Acta, Biomembranes, 2016. **1858**: p. 1926-1934.
39. Eichner, A.S., S., Dobner, B., Hauß, T., Schroeter, A., Neubert, R. H. H., *Determination of the position of long-chain ω-acyl ceramide [EOS] within the long-periodicity phase in stratum corneum lipid model membranes.* Biochimica et Biophysica Acta, 2016.
40. Mak, V.H.W., R.O. Potts, and R.H. Guy, *Oleic acid concentration and effect in human stratum corneum: non-invasive determination by attenuated total reflectance infrared spectroscopy in vivo.* Journal of Controlled Release, 1990. **12**(1): p. 67-75.
41. Francoeur, M.L., G.M. Golden, and R.O. Potts, *Oleic acid: its effects on stratum corneum in relation to (trans)dermal drug delivery.* Pharm Res, 1990. **7**(6): p. 621-7.
42. Ongpipattanakul, B., et al., *Phase-Separation of Oleic-Acid in the Stratum-Corneum Lipids.* Journal of Investigative Dermatology, 1991. **96**(4): p. 619-619.
43. Ongpipattanakul, B., et al., *Evidence that oleic acid exists in a separate phase within stratum corneum lipids.* Pharm Res, 1991. **8**(3): p. 350-4.
44. Santoyo, S., Arellano, A., Ygartua, P., Martin, M., *Penetration enahncer effects on the in-vitro percutaneous absorption of piroxicam through rat skin.* International Journal of Pharmaceutics, 1995. **117**(2): p. 219-224.
45. Sato, K., Sugibayashi, K., Morimoto, Y., *Effect and mode of action of aliphatic esters on the invitro skin permeation of nicorandil.* international Journal of Pharmaceutics, 1988. **43**(1-2): p. 31-40.
46. Barry, B.W., *Lipid-protein-partitioning theory of skin penetration enhancement.* Journal of Controlled Release, 1991. **15**(3): p. 237-248.
47. Pham, Q.D., Björklund, S., Engblom, J., Topgaard, D., Sparr, E., *Chemical penetration enhancers in stratum corneum- Relation between molecular effects and barrier function.* Journal of Controlled Release, 2016. **232**: p. 175-187.
48. Arellano, A., Santoyo, S., Martin, C., Ygartua, P., *Influence of propylene glycol and isopropyl myristate on the in vitro percutaneous penetration of diclofenac sodium from carbopol gels.* European Journal of Pharmaceutical Sciences, 1998. **7**(2): p. 129-135.
49. Leopold, C.S., Lippold, B. C., *An attempt to clarify the mechanism of the penetration enhancing effects of lipophilic vehicles with differential scanning calorimetry (DSC).* Journal of Pharmacy and Pharmacology, 1995. **47**(4): p. 276-281.
50. Brinkmann, I., Mueller-Goymann, C. C., *An attempt to clarify the influence of glycerol, propylene glycol, isopropyl myristate and a combination of propylene glycol and isopropyl myristate on human stratum corneum.* Pharmazie, 2005. **60**(3): p. 215-220.
51. Engelbrecht, T.N., Demé, B., Dobner, B., Neubert, R. H. H., *Study of the Influence of the Penetration Enhancer Isopropyl Myristate on the Nanostructure of Stratum Corneum Lipid Model Membranes Using Neutron Diffraction and Deuterium Labelling.* Skin Pharmacology and Physiology, 2012. **25**(4): p. 200-207.
52. Harroun, T.A., Wignall, G. D., Katsaras, J., *Neutron Scattering for Biology*. Neutron Scattering in Biology : Techniques and Applications, ed. J. Fitter, Gutberlet, T., Katsaras, J. 2006, Berlin Heidelberg: Springer-Verlag.
53. Dachs, H., *Principles in Neutron Diffraction*. Topics in Current Physics, Neutron Diffraction, ed. H. Dachs. 1978, Berlin Heidelberg: Springer-Verlag.
54. Willis, B.T.M., Carlile, C. J., *Neutron properties*. Experimental Neutron Scattering. Vol. 1. 2009, Oxford, Great Britain: Oxford University Press. 325.

55. Zajac, W., Gabrys, B. J., *An introduction to neutron scattering*. Applications of neutron scattering to Soft condensed matter, ed. B.J. Gabrys. Vol. 1. 2000, Amsterdam, Netherlands: Gordon and Breach Science Publishers. 1-26.
56. Kessner, D., Kiselev, M., Dante, S., Hauss, T., Lersch, P., Wartewig, S., Neubert, R. H. H., *Arrangement of ceramide [EOS] in a stratum corneum lipid model matrix: new aspects revealed by neutron diffraction studies.* European Biophysics Journal, 2008. **37**(6): p. 989-999.
57. Kessner, D., Mikhail A., Hauss, T., Dante, S., Wartewig, S., Neubert, R. H. H., *Localisation of partially deuterated cholesterol in quaternary SC lipid model membranes: a neutron diffraction study.* European Biophysics Journal, 2008. **37**(6): p. 1051-1057.
58. Mojumdar, E.H., Groen,D., Gooris, G. S., Barlow, D. J., Lawrence, M. J., Demé, B., Bouwstra, J. A., *Localization of Cholesterol and Fatty Acid in a Model Lipid Membrane: A Neutron Diffraction Approach.* Biophysical Journal, 2013. **105**: p. 911-918.
59. Engelbrecht, T.N., Schroeter, A., Hauss, T., Neubert, R. H. H., *Lipophilic penetration enhancers and their impact to the bilayer structure of stratum corneum lipid model membranes: Neutron diffraction studies based on the example Oleic Acid.* Biochimica et Biophysica Acta, Biomembranes, 2011. **1808**(12): p. 2798-2806.
60. Rehfeld, S.J., Elias, P. M., *Mammalian Stratum Corneum contains Physiological Lipid Thermal Transitions.* The Journal of Investigative Dermatology, 1982. **79**(1): p. 1-3.
61. Engelbrecht, T., Hauß, T., Süß, K., Vogel, A., Roark, M., Feller,S. C., Neubert, R. H. H., Dobner, B., *Characterisation of a new ceramide EOS species: synthesis and investigation of the thermotropic phase behaviour and influence on the bilayer architecture of stratum corneum lipid model membranes.* Soft Matter, 2011. **7**: p. 8998-9011.
62. Seul, M., Sammon, M.J., *Preparation of surfactant multilayer films on solid substrates by deposition from organic solution.* Thin Solid Films, 1990. **185**(2): p. 287-305.
63. Worchester, D.L., Franks, N.P., *Structural Analysis of hydrated egg lecithin and cholesterol bilayers, II. Neutron Diffraction.* Journal of Molecular Biology, 1976. **100**(3): p. 359-378.
64. Wiener, M.C., White, S. H., *Fluid bilayer structure determination by the combined use of x-ray and neutron diffraction.* Biophysical Journal, 1991. **59**: p. 174-185.
65. Schoneborn, B.P., Nunes, A.C., *Neutron Scattering.* Annual Review of Biophysics and Bioengineering, 1972. **1**: p. 529-552.
66. Zentrum, H.M.-L., *BIODIFF: Diffractometer for large unit cells.* Journal of large-scale research facilities, 2015. **1**(A2): p. 1-4.
67. Casadei, C.M., Gumiero, A., Metcalfe, C. L., Murphy, Em J., Basran, J., Concilio, M. G., Reixeira, S. C. M., Schrader, T. E., Fielding, A. J., Ostermann, A., Blakeley M. P., Raven, E. L. Moody, P. C. E., *Neutron cryo-crystallography captures the protonation state of ferryl heme in a peroxidase.* Science, 2014. **345**(6193): p. 193-197.
68. Coates, L., Tomanicek, S., Schrader, T. E., Weiss, K. L., Ng, J. D., Juettner, P., Ostermann, A., *Cryogenic neutron proetein crystallography: routine methods and potential benefits.* Journal of Applied Crystallography, 2014. **47**(4): p. 1431-1434.
69. Yokoyama, T., Ostermann, A., Mizuguchim M., Niimura, N., Schrader, T. E., Tanaka, I., *Crystallization and preliminary neutron diffraction experiment of human farnesyl pyrophosphate synthase complexed with risedronate.* Acta Crystallographica Section F: Structural Biology and Crystallization Communications, 2014. **70**(4): p. 470-472.
70. Bryan, T., Gonzalez, J. M., Bacik, J. P. DeNunio, N. J., Unkefer, C. J., Schrader, T. E., Ostermann, A., Dunaway-Mariano, D., Allen, K. N., Fisher, S. Z., *Neutron diffraction studies towards deciphering the protonation state of catalytic residues in the bacterial KDN9P phosphatase.* Acta Crystallographica Section F: Structural Biology and Crystallization Communications, 2013. **69**(9): p. 1015-1019.
71. Ostermann, A., Schrader, T, *BIODIFF- diffractometer for large unit cells*. Experimental facilities; Heinz Maier-Leibnitz Zentrum, ed. R. Bruchhaus, Carsughi, F.,

Hesse, C., Link, P., Lommatzsch, I., Neuhaus, J., Voit, A. 2013, Garching, Germany: Forschungs-Neutronenquelle Heinz Maier-Leibnitz (FRM II).
72. Ostermann, A., Schrader, T. E., *BioDiff: The new diffractometer for crystals with large unit cells*, in *MLZ report 2011-2013*, R. Bucher, Lommatzsch, I., Editor. 2014: Garching, Germany.
73. Ostermann, A., Schrader, T. E., *Schematic view of BIODIFF*. 2013.
74. Dante, S., Hauss, T., Dencher, N. A., *Insertion of Externally Administered Amyloid β Peptide 25-35 and Perturbation of Lipid Bilayers.* Biochemistry, 2003. **42**(46): p. 13667-13672.
75. Kiselev, M.A., Ryabova, N. Y., Balagurov, A. M., Dante, S., Hauss, T., Zbytovska, J., Wartewig, S., Neubert, R. H. H., *New insights into the structure and hydration of a stratum corneum lipid model membrane by neutron diffraction.* European Biophysics Journal, 2005. **34**: p. 1030-1040.
76. Franks, N.P., Lieb, W.R., *The Structure of Lipid Bilayers and the Effects of General Anaesthetics.* Journal of Molecular Biology, 1979. **133**: p. 469-500.
77. Cser, F., *About the Lorentz correction used in the interpretatin of small angle X-ray scattering data of semicrystalline polymers.* Journal of Applied Polymer Science, 2001. **80**(12): p. 2300-2308.
78. Nagle, J.F., Tristam-Nagle, S., *Structure of lipid bilayers.* Biochimica et Biophysica Acta, 2000. **1469**: p. 159-195.
79. Sears, V.F., *Neutron scattering lengths and cross section.* Neutron News, 1992. **3**(3): p. 26-37.
80. Fenske, D.B., Thewalt, J. L., Bloom, M., Kitson, N., *Models of Stratum Corneum Intercellular Membranes: ^{2}H NMR of Macroscopically Oriented Multilayers.* Biophysical Journal, 1994. **67**: p. 1562-1573.
81. Huster, D., Arnold, K., Gawrisch, K., *Influence of docosahexaenoic acid and cholesterol on lateral lipid organization in phospholipid membranes.* Biochemistry, 1998. **37**: p. 17299-17308.
82. Macho, V., Brombacher, L., Spiess, H. W., *The NMR-WEBLAB: An Internet Approach to NMR Lineshape Analysis.* Applied Magnetic Resonance, 2001. **20**: p. 405-432.
83. de Jager, M.W., Gooris, G. S., Dolbnya, I. P., Ponec, M., Bouwstra, J. A., *Modelling the stratum corneumlipid organisation with synthetic lipid mixtures: the importance of synthetic ceramide composition.* Biochimica et Biophysica Acta, 2004. **1684**: p. 132-140.
84. Groen, D., Gooris, G. S., Barlow, D. J., Lawrence, M. J., van Mechelen, J. B., Demé, B., Bouwstra, J. A., *Disposition of ceramide in model lipid membranes determined by neutron diffraction.* Biophysical Journal, 2011. **100**(6): p. 1481-1489.
85. Petrache, H.I., Dodd, S. W., Brown, M. F., *Area per lipid and Acyl Length Distribution in Fluid Phosphatidylcholines Determined by ^{2}H NMR Spectroscopy.* Biophysical Journal, 2000. **79**: p. 3172-3192.
86. Small, D.M., *The physical chemistry of lipids*. Handbook of Lipid Research, ed. D.J. Hanahan. 1986, New York: Plenum Press.
87. Kitson, N., Thewalt, J., Lafleur, M., Bloom, M., *A model membrane approach to the epidermal permeability barrier.* Biochemistry, 1994. **33**: p. 6707-6715.
88. Leung, S.S., Busto, J. V., Keyvanloo, A., Goni, F. M., Thewalt, J., *Insights into sphingolipid miscibility: separate observation of sphingomyelin and ceramide N-acyl chain melting.* Biophysical Journal, 2012. **103**: p. 2465-2474.
89. Brief, E., Kwak, S., Cheng, J. T., Kitson, N., Thewalt, J., Lafleur, M., *Phase behavior of an equimolar mixture of N-palmitoyl-D-erythro-sphingosine, cholesterol, and palmitic acid, a mixture with optimized hydrophobic matching.* Langmuir, 2009. **25**: p. 7523-7532.
90. Stahlberg, S., Skolova, B., Madhu, P. K., Vogel, A., Vavrova, K., Huster, D., *Probing the role of the ceramide acyl chain length and sphingosine unsaturation in model skin barrier lipid mixtures by 2H solid-state NMR spectroscopy.* Langmuir, 2015. **32**: p. 4906-4915.

91. Rowat, A.C., Kitson, N., Thewalt, J. L., *Interactions of oleic acid and model stratum corneum membranes as seen by 2H NMR.* International Journal of Pharmaceutics, 2006. **307**: p. 225-231.
92. Wittebort, R.J., Olejniczak, E. T., Griffin, R. G., *Analysis of deuterium nuclear magnetic resonance line shapes in anisotropic media.* The Journal of Physical Chemics, 1987. **86**(10): p. 5411-5420.
93. Batchelder, L.S., Sullivan, C. E., Jelinski, L. W., Torchia, D. A., *Characterization of leucine side-chain reorientation in collagen- fibrils by solid-state 2H NMR.* Proceedings of the National Academy of Sciences of the United States of America, 1982. **79**: p. 386-389.
94. Huster, D., *Investigations of the structure and dynamics of membrane-associated peptides by magic angle spinning NMR.* Progress in Nuclear Magnetic Resonance Spectroscopy, 2005. **46**: p. 79-107.
95. Schmidt, P., Thomas, L., Müller, P., Scheidt, H. A., Huster, D., *The G protein-coupled neuropeptide Y receptor type 2 is highly dynamic in lipid membranes as revealed by solid-state NMR spectroscopy.* Chemistry 2014. **20**: p. 4986-4992.
96. Huster, D.X., L.; Hong, M. , *Solid-state NMR investigation of the dynamics of soluble and membrane-bound colicin Ia channel-forming domain.* Biochemistry, 2001. **40**: p. 7662-7674.
97. Ouimet, J., Lafleur, M., *Hydrophobic match between cholsterol and saturated fatty acid is required for the formation of lamellar liquid ordered phases.* Langmuir, 2004. **20**(18): p. 7474-7481.